VALIDATION OF NEPTUNE_CFD 1.0.8 FOR ADIABATIC BUBBLY FLOW AND BOILING FLOW

A. Douce[1], S. Mimouni[1], M. Guingo[1], C. Morel[2], J. Laviéville[1], C. Baudry[1]

[1]Electricité de France, Chatou, FRANCE. alexandre.douce@edf.fr
[2]Commissariat à l'Energie Atomique, Grenoble, FRANCE.

Abstract

The NEPTUNE_CFD code, which is based on an Eulerian two-fluid model, is mainly focused on Nuclear Reactor Safety applications involving two-phase flows, like Pressurized Thermal Shock and Departure from Nucleate Boiling (DNB). Since the maturity of two-phase CFD has not reached yet the same level as single phase CFD, an important work of model development and thorough validation is needed. Many of these applications involve bubbly and boiling flows, and therefore it is essential to validate the software on such configurations. In particular, this is crucial for applications to flow in PWR fuel assemblies, including studies related to DNB. Four experiments were selected for the validation. The Liu and Bankoff experiment (1993) and the Bel F'Dhila experiment (1991) for adiabatic air-water bubbly flow. The DEBORA (Manon, 2000) and the ASU (Hasan, 1990) facilities for boiling flows. A key feature of this work is that all these computations were performed with a single standard version (1.0.8) of NEPTUNE_CFD, and with a single and consistent set of models. Comparisons with experimental data show that NEPTUNE_CFD has captured experimental profiles with reasonable accuracy for dynamical quantities and void fraction. Improvement must be done for the prediction of the bubbles size distribution.

1 INTRODUCTION

The NEPTUNE_CFD code, which is based on an Eulerian two-fluid model, is developed within the framework of the NEPTUNE project (Guelfi, 2007), financially supported by CEA (Commissariat à l'Énergie Atomique), EDF, IRSN (Institut de Radioprotection et de Sûreté Nucléaire) and AREVA-NP. NEPTUNE_CFD is mainly focused on Nuclear Reactor Safety applications involving two-phase flows, like two-phase Pressurized Thermal Shock (PTS) and Departure from Nucleate Boiling (DNB). Since the maturity of two-phase CFD has not reached yet the same level as single phase CFD, an important work of model development and thorough validation is needed, as stated for example in NEA/CSNI Writing Group dedicated to the "Extension of CFD Codes to Two-Phase Flow Safety Problems" (Bestion, 2009). Many of these applications involve bubbly and boiling flows, and therefore it is essential to validate the software on such configurations. In particular, this is crucial for applications to flow in PWR fuel assemblies, including studies related to DNB. This work aims at presenting the present status of NEPTUNE_CFD validation in this area, as a step in an iterative process of improvement.

To this end, this paper presents NEPTUNE_CFD code validation against four test cases based on experimental results. These data have been selected to allow separate effects validation. The adequacy of the measured quantities and the corresponding basic model of the CFD code to validate is underlined in each case. The selected test cases are the following. The Liu and Bankoff experiment (1993) is an adiabatic air-water bubbly flow inside a vertical pipe. It allows to validate forces applied to the bubbles. The Bel F'Dhila (1991) experiment is an adiabatic bubbly air-water flow inside a sudden pipe expansion. It allows to validate the dynamic models and turbulence. The DEBORA (Manon, 2000) and the ASU (Arizona State University, Hasan 1990) facilities provide results for boiling flows inside a vertical pipe. The working fluid is refrigerant R12 for DEBORA and R113 for ASU. Both allow to validate the nucleation modeling on a heated wall, and ASU allows also the validation of the two-phase wall function (Mimouni, 2009).
The paper is organised as follows. In section 2, the main principles of the modelling are described without any equation nor detail, in the view to give to the reader a picture of the context, in other

words, to introduce the validation. In the next four sections, the validation cases are presented, with three sub-sections: description of the test case, computational representation and results.

2 MODEL DESCRIPTION

2.1 Two-phase model and solver

NEPTUNE_CFD is a three dimensional two-fluid code developed more especially for nuclear reactor applications. This code is based on the classical two-fluid one pressure approach (Ishii, 1975), (Delhaye, 1981), and is able to simulate multi-component multiphase flows by solving a set of three balance equations for each field (fluid component and/or phase) (Méchitoua, 2003), (Guelfi, 2007), (Mimouni, 2008, 2009). These fields can represent many kinds of multiphase flows: distinct physical components (e.g. gas, liquid and solid particles); thermodynamic phases of the same component (e.g.: liquid water and its vapour); distinct physical components, some of which split into different groups (e.g.: water and several groups of different diameter bubbles); different forms of the same physical components (e.g.: a continuous liquid field, a dispersed liquid field, a continuous vapour field, a dispersed vapour field).

The discretization follows a 3D full unstructured finite volume approach, with a collocated arrangement of all variables. Numerical consistency and precision for diffusive and advective fluxes for nonorthogonal and irregular cells are taken into account through a gradient reconstruction technique. Convective schemes for all variables, except pressure, are centered/upwind scheme. Velocities components can be computed with a full centered scheme. The solver is based on a pressure correction fractional step approach. Gradients are calculated at second order for regular cells and at first order for highly irregular cells.

A set of local balance equations for mass, momentum and energy is written for each phase. These balance equations are obtained by ensemble averaging of the local instantaneous balance equations written for the two phases. When the averaging operation is performed, the major part of the information about the interfacial configuration and the microphysics governing the different types of exchanges is lost. As a consequence, a number of closure relations must be supplied for the total number of equations (the balance equations and the closure relations) to be equal to the number of unknown fields. We can distinguish three different types of closure relations: those which express the inter-phase exchanges (interfacial transfer terms), those which express the intra-phase exchanges (molecular and turbulent transfer terms) and those which express the interactions between each phase and the walls (wall transfer terms) (Mimouni, 2008).

2.2 Computional strategy

An essential point of this work is that all computations presented below were performed with a single standard version (1.0.8) of NEPTUNE_CFD, and with a single and consistent set of models, avoiding case-dependent “tuning” of the modeling. Particularly, we do not specifically optimize the coefficients and modeling of the momentum transfer terms to get results as good as possible.

In the scope of the presented cases, incompressibility assumption is used for the both phases.

The turbulence of the continuous phase is treated with a RANS approach, namely a Reynolds Stress Model (RSM). The interfacial transfer of momentum, is assumed to be the sum of four forces: the averaged drag from Ishii (1990), added mass from Zuber (1964), lift from Tomiyama (1998) and turbulent dispersion from Lance *et al.* (1994).

The wall transfer model for nucleate boiling follow the analysis of Kurul *et al.* (1990), the boiling heat flux is split into three terms:

- single phase flow convective heat flux q_c at the fraction of the wall area unaffected by the presence of bubbles,
- quenching heat flux q_q where bubbles departure bring cold water in contact with the wall periodically,
- vaporisation heat flux q_e needed to generate the vapour phase.

The bubble detachment diameter is given by the correlation from Unal *et al.* (1977). The Unal's correlation is valid for subcooled liquid but has been extended to saturated liquid. In order to take into account the influence of bubbles in the near wall area, a modified logarithmic law of the wall was introduced (Mimouni, 2008).

Furthermore, the interfacial area model of Ruyer *et al.* (2007) has been used in the computations. This model makes it possible to simulate a polydispersion for the size of the bubbles by representing the bubble-size distribution through the use of a quadratic law.

The time step chosen is time-dependent, with a maximum CFL number set to 1. For investigation of flow solver convergence, the gas holdup and the global mass balances for both phases were defined as monitored target variables.

The NEA/CSNI Best Practice Guidelines were followed as much as possible, especially in the mesh generation process by keeping acceptable quality for the grids, by exploring the grid convergence, and also by assessing the numerical convergence.

3 ADIABATIC BUBBLY FLOW IN A VERTICAL PIPE. LIU AND BANKOFF TEST CASE

3.1 Description of the test case

In this section, we evaluate the modelling capabilities to simulate an upward bubbly flow in adiabatic conditions (Liu, 1993). We consider an experiment featuring an adiabatic air water bubbly flow. The test case facility was a Z = 2800 mm long, vertical smooth acrylic tubing, with inside diameter of D = 38 mm.
The uncertainty for flow conditions is within ±5%. The consistency of liquid velocity is within ±1.5%.

3.2 Computational representation

A uniform axial liquid profile is imposed at the inlet and is equal to 1.138 m/s. A uniform axial gas profile is imposed at the inlet and is equal to 1.333 m/s. The void fraction at the inlet is 0.045. The bubble diameter is set to 2.5 mm at the inlet in accordance with experimental observations; this diameter is used to initialize the boundary condition of the interfacial area model of Ruyer *et al.* (2007).

The flow is assumed to be axisymmetric therefore a two-dimensional axisymmetric meshing is used. Computations have been performed on three grids. Their characteristics are summarized in Table 1.

Number of cells	Grid level 1	Grid level 2	Grid level 3
Radial direction	20	30	40
Axial direction	400	300	800

Table 1: Characteristics of the grids used in the Liu and Bankoff test case.

3.3 Results

At the measuring station (Z/D = 36), we compare numerical results against experimental data for the void fraction (Figure 1) and the axial liquid velocity (Figure 2). The results obtained by using the two level 2 and level 3 of grid refinement, although not strictly identical, are reasonably close.

Figure 1 and Figure 2 show that the simulation results are in quite reasonable agreement with the experimental data. However, in this case, the use of a polydisperse approach does not improve the results comparing to a monodisperse approach (Mimouni, 2008). The computed void fraction profile plotted in Figure 1 does not have the measured shape: the position of peak of void fraction is not reproduced. In fact, small bubbles move towards the wall, whereas large bubbles move towards the core of the flow. This migration is mainly a consequence of the lift force. Thus, bubble diameter have to be computed accurately. But the bubble diameter depends on coalescence and break-up phenomena, for which the modelling should be investigated more systematically. Moreover, this migration depends

on uncontrolled parameters like the bubble shape, the liquid turbulence, the bubbles collective effects and so on (Cheung, 2007)…

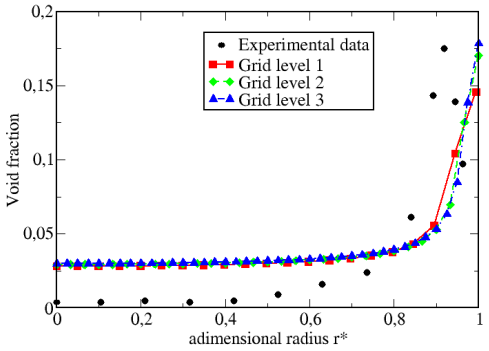

Figure 1: Radial profile of void fraction.

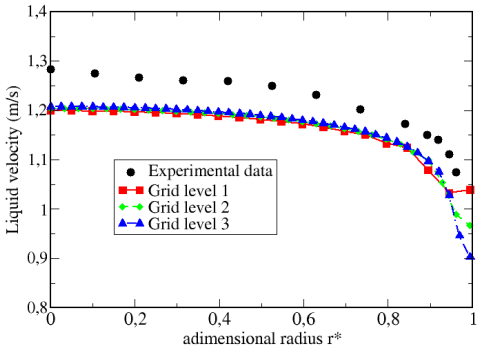

Figure 2: Radial profile of axial liquid velocity.

4 ADIABATIC BUBBLY FLOW IN SUDDEN PIPE EXPANSION. BEL F'DHILA EXPERIMENT

4.1 Description of the test case

Bel-Fdhila (Bel-Fdhila, 1991) (Bel-Fdhila and Simonin, 1992) investigated experimentally several upwards bubbly flows in a vertical pipe with a sudden expansion. The total length of the pipe was equal to 14 meters. The bottom part of the tube had a length equal to 9 meters and an internal diameter equal to 50 mm, the top part of the tube (5 m length) having an internal diameter equal to 100 mm. The fluids used were water and air under atmospheric pressure and ambient temperature. Six measuring sections were located upstream and downstream of the singularity. The first measuring section was located two centimetres before the singularity, the other five were located at 7, 13, 18, 25 and 32 cm above the singularity. In each measuring section, the radial profile of the void fraction was measured by means of a single optical probe and two components of the liquid velocity were measured by means of a hot film anemometer. The time-averaged components of this velocity field and three components of the liquid Reynolds stress tensor were deduced (the flow being assumed axisymmetric). The bubble size was not measured in the experiment. According to the author, the observed bubble diameter was equal to a few millimetres, the bubbles remaining relatively small due to the strong turbulence existing in the liquid phase. Therefore, in our computations, a bubble diameter was fixed to 2 mm at inlet. This diameter is used to initialize the boundary condition at the inlet of the interfacial area model of Ruyer *et al.* (2007).

The flow studied here is characterized by the liquid and gas superficial velocities and the area-averaged void fraction in the two sections given in table 2. It can be noted that the averaged void fraction for this test is 12 %.

Internal Diameter (mm)	J_L (m/s)	J_G (m/s)	$<\alpha>_2$
50	1.57	0.3	0.12
100	0.39	0.075	0.0903

Table 2: Simulated test case

4.2 Computational representation

In our simulations, only a small part of the tube, containing the singularity and the six measuring sections, was reproduced. The radial profiles of the void fraction and the liquid mean and fluctuating velocities measured upstream of the singularity were used as inlet conditions. The length of the computational domain is equal to 38 cm. For the facility geometry, radial symmetry has been assumed,

so that the numerical simulations could be performed on a angular sector of the pipe with symmetry boundary conditions at both sides. A hierarchy of three numerical meshes was constructed, where the number of cells has been increased by a factor of 2 from a coarser to a finer mesh (grid level 1: 4864 cells, grid level 2: 19456 cells, grid level 3: 77824 cells).

4.3 Results

For all mesh levels, reliable converged solutions have been reached. In Figures 3 to 6 numerical simulations give almost grid independent results for all meshes.

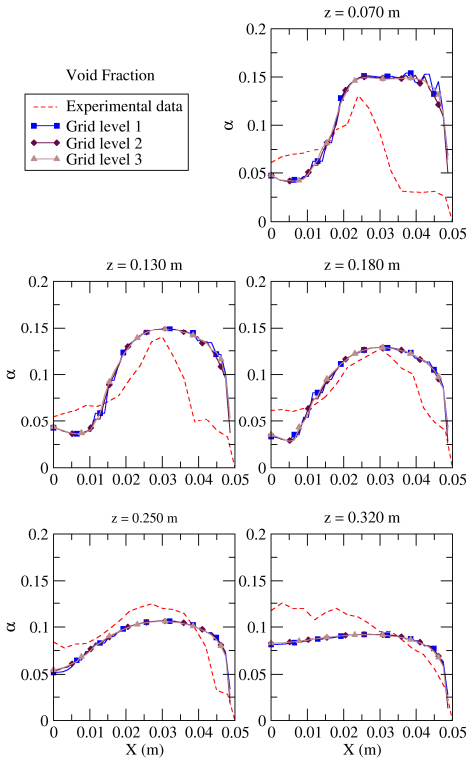

Figure 3: Radial profile of void fraction.

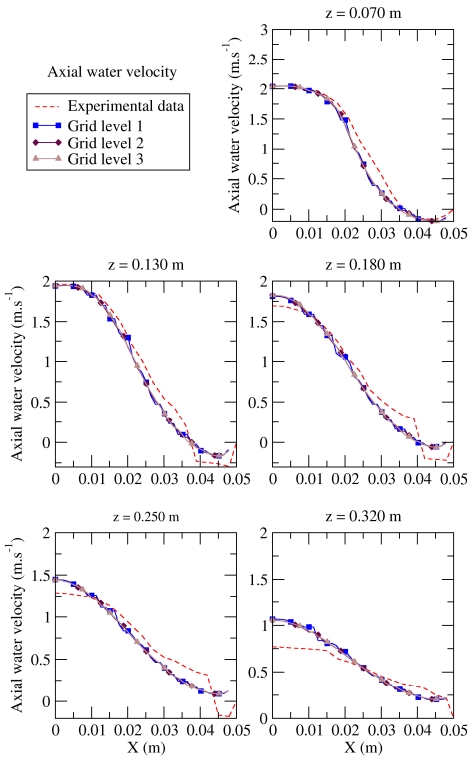

Figure 4: Radial profile of axial liquid velocity.

For void fraction, the comparison with the measurements (Figure 3) shows a qualitatively correct behaviour and have been improved as compared to (Morel, 2004) and (Cokljat, 2006). However, the profiles show that too many bubbles are staying in the recirculation area (Figure 3, z = 0.07 m) and that the void fraction at the axis of the pipe is globally underestimated.

Globally, polydisperse approach does not improve the results comparing to a monodisperse approach (Mimouni, 2008), but unlike (Lance, 1994), (Morel, 2004), (Cokljat, 2006), and (Mimouni, 2008) the lift force acting on bubbles was not discarded, and no spurious behaviour was observed near the wall.

Figures 4 and 5 show that computed axial and radial mean liquid velocity profiles are quite close to the measurements which means that the recirculation zone is well captured. Nevertheless, in the axis of the pipe we can see that the predictions for the water axial velocity are less accurate for planes which are more distant from the inlet.

We have obtained satisfactory results for turbulent kinetic energy (Figure 6) although the turbulent kinetic energy is overestimated at a radius of 0.02 m and underestimated near the wall.

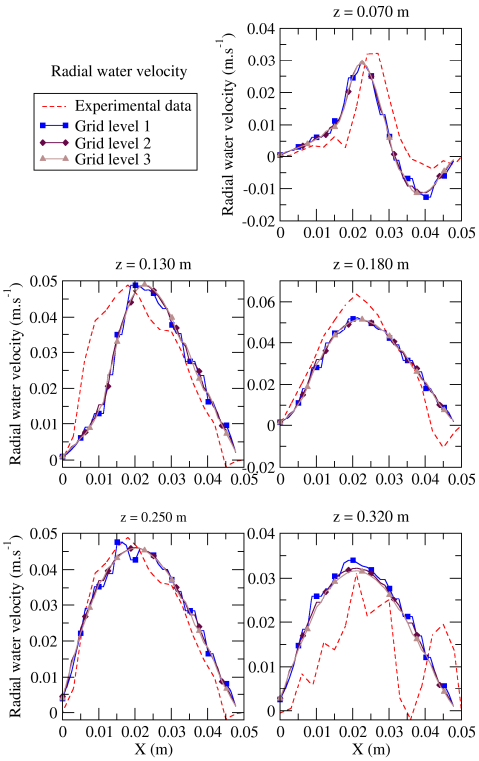

Figure 4: Radial profile of radial liquid velocity.

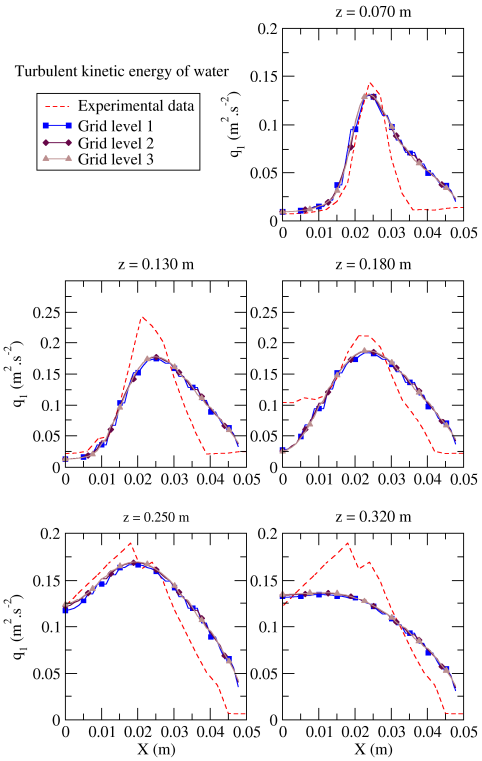

Figure 6: Radial profile of turbulent kinetic energy.

5 BUBBLY FLOW IN A VERTICAL PIPE. THE DEBORA FACILITY.

5.1 Description of the test case

The DEBORA experiment has been performed at the CEA-Grenoble (Manon, 2000). It is devoted to the study of boiling bubbly flows in a vertical pipe with a circular cross-section. The working fluid is R12; it is injected as a subcooled liquid at the bottom of the pipe. The 5 meter high pipe is divided into three parts: first, an adiabatic inlet section (0.5 m); then, a 3.5 meter heated section and finally an adiabatic outlet section (0.5 m). At the end of the heated section, radial profiles of the following quantities are measured: steam axial velocity, void fraction and liquid temperature, as well as properties related to the bubble-size distribution: the interfacial area concentration and the Sauter mean bubble diameter (Morel, 2010). The test case simulated (labeled G2P26W16Te70) is performed under the operating conditions presented in table 3:

Test pressure P	26.15 bar
Inlet mass flow rate G	1985 kg/m^2/s
Wall heat flux density	73890 W/m^2
Inlet liquid temperature	70.53 °C

Table 3: Operating conditions of the simulated test-case of the DEBORA experiment.

The measurement uncertainties were evaluated by Manon (2000) to be ±0.02 on the void fraction, ±10% on the volumetric interfacial area and ±12% on the Sauter mean diameter. We have also noted an uncertainty on the liquid temperature equal to ±0.2 °C.

5.2 Computational representation

The flow is assumed to be axisymmetrical: the computations are thus carried out in a two-dimensional axisymmetric domain (i.e. the grid is three-dimensional, with one cell in the azimuthal direction). For these computations, two meshes have been constructed with different refinements: The coarser one (denoted as “grid level 1”) counts 800 cells, while the finer (“grid level 2”) counts 8 000 cells. Their detailed characteristics can be found in table 4:

	Grid level 1	Grid level 2
Total number of cells	800	8 000
Number of cells in the radial direction	10	20
Number of cells in the axial direction	80	400
Cell size in the radial direction	0.96 mm	0.48 mm
Cell size in the axial direction	6.25 cm	1.25 cm

Table 4: Characteristics of the grids used in the DEBORA simulations

5.3 Results

The steady state is reached after approximately 30 s simulation time. Figures 7 to 11 compare the computed radial profiles of the following quantities to the experiments: the void fraction, the liquid temperature, the bubble Sauter mean diameter, the interfacial area concentration and the interfacial axial velocity.

It can be observed in Figures 7 to 11 that the results obtained by using the two grid refinements, although not strictly identical, are reasonably close. The radial profiles of the mean interfacial velocity and of the interfacial area concentration are satisfactorily retrieved by the simulation. The computed radial profile of the interfacial area concentration compares favorably with the experimental data, suggesting the polydispersion model of Ruyer *et al* (2007), associated with a second-order turbulence model, can successfully reproduce the main features of the bubble-size distribution for this test-case.

Concerning the liquid temperature, a difference onto the heated wall is observed, but its magnitude remains small with 2 Kelvin.

In the other hand, the void fraction presents a discrepancy in the vicinity of the wall. The profile illustrates that vapour bubbles are nucleated onto the heated wall surface and condense in the subcooled liquid in the core of the flow. The liquid temperature profile is the combination of several phenomena: the liquid near the wall is heated by the single phase flow convective heat flux plus the quenching heat flux; bubbles condense in the subcooled liquid in the core of the flow and heat the liquid; the molecular and turbulent heat fluxes inside the liquid phase modify the temperature profile.

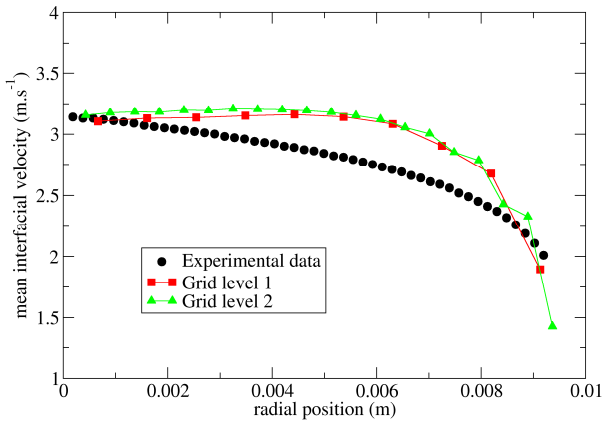

Figure 7: Radial profile of the mean interfacial velocity.

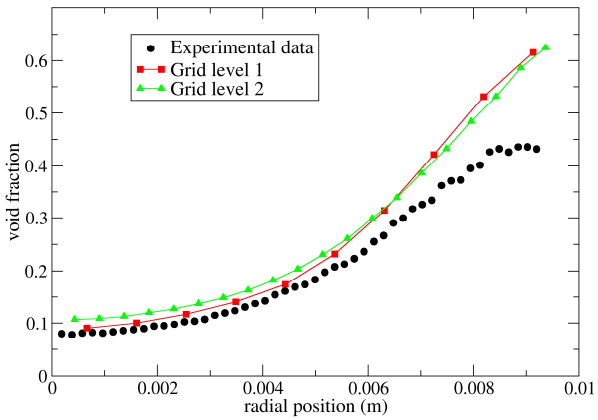

Figure 8: Radial profile of the void fraction.

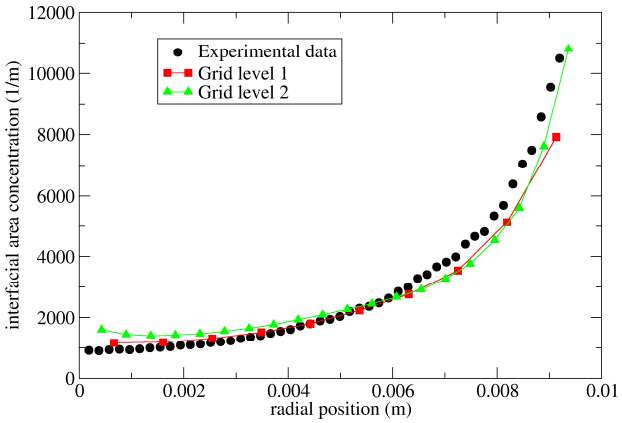

Figure 9: Radial profile of the interfacial area concentration.

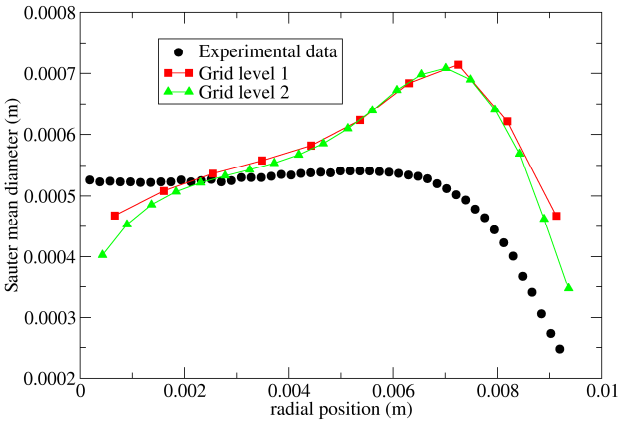

Figure 10: Radial profile of the Sauter mean diameter.

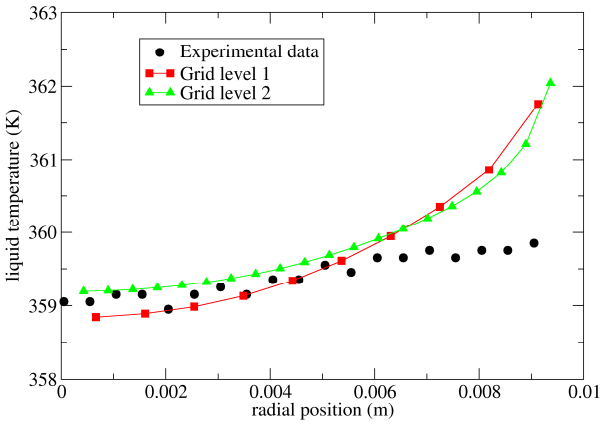

Figure 11: Radial profile of the liquid temperature.

6 BOILING FLOW IN AN ANNULAR VERTICAL PIPE. THE ASU TEST CASE

6.1 Description of the test case

The Arizona State University (ASU) experiment is described in (Hasan, 1990) and (Roy, 1993) for two-phase boiling flow measurements. The test section of the ASU experiment consists of a vertical annular channel with a heated inner wall and an insulated outer wall. The inner tube is made of 304 stainless steel (inlet diameter = 14.6 mm, outlet diameter = 15.9 mm) and the outer pipe of transparent Pyrex glass (i. d. = 38.1 mm, o. d. = 47 mm) except for a 0.496 m long measurement section which is made of quartz (i.d. = 37.7 mm, o.d. = 41.7 mm). The inner tube is resistively heated, the upper 2.75 m of the 3.66 m long test section being the heated length. The lower 0.91 m serves as the hydrodynamic entrance length. The working fluid is refrigerant 113 (R113).

When the inner wall heating is sufficiently high, heterogeneous nucleation appears onto this wall surface. As the inlet liquid is subcooled, the bubbles condense into the colder liquid when they are far from the inner wall layer. According to Roy *et al.* (Roy, 1993), a two layer is observed: a boiling bubbly layer adjacent to the heated wall and an outer all liquid region. A dual-sensor optical fibre probe and a microthermocouple were installed diametrically opposite each other in the measurement section. The measurement plane was approximately located at 1.94 m downstream of the beginning of the heated length. The dual-sensor optical fibre probe was used to measure the radial profiles of the different quantities characterizing the dispersed phase (void fraction, bubble axial velocity and bubble chord length). The bubble chord length distribution allows to compute the bubble diameter distribution, hence the local interfacial area concentration, by making several assumptions (see Roy *et al.*(1993) for more explanations). However, these authors conclude that further work is needed before the local interfacial area concentration can be determined with confidence.

We have the radial profiles of the void fraction, the mean axial liquid velocity, and the mean liquid temperature for two different experimental cases we name TP5 and TP6. Only TP5 is presented in the scope of this paper. The controlling parameters for this case are indicated in table 5 below.

Case	Pressure (bar)	Wall heat flux (W/m^2)	Inlet mass flow rate (kg/m^2s)	Inlet temperature (°C)
Tp5	2.69	95	784	50.2

Table 5: Experimental conditions retained for the ASU test case.

6.2 Computational representation

The length of the ASU computational domain is equal to 3.30 m and the last 2.39 m length are heated. The flow is assumed to be axisymmetric therefore a two-dimensional axisymmetric computation grid has been used. Computations have been performed with two grids: a coarse grid (20 cells in the radial direction and 200 cells in the axial direction), and a fine grid (30 cells in the radial direction and 200 cells in the axial direction). Figures 12 to 14 show that the results are close for the two grids.

6.3 Results

The steady state is reached after approximately 10 s simulation time. Figures 12 to 14 compare the computed radial profiles of the following quantities to the experiments: the void fraction, the liquid velocity and the liquid temperature.

It can be observed in Figures 12 to 14 that the results obtained by using the two grid refinements are not strictly identical, but are reasonably close, except for liquid velocity near the inner wall. This point must be further investigated. The computed radial profile of the void fraction compares favorably with the experimental data (Figure 12). In the other hand, the liquid mean axial velocity shows a discrepancy in the side of the heated wall (Figure 13). Compared to the results of Mimouni *et al* (Mimouni, 2009), this profile in the vicinity of the inner tube are worse, than those computed with a constant bubble diameter, fixed to 1.2 mm in accordance with experimental observations. In fact, the computed bubble diameter near the heated wall is underestimated (0.6 mm instead of 1.2

mm) and consequently, the wall functions dedicated to boiling flows tend to the classical single-phase wall function which are less adapted to this case.
The liquid temperature is underestimated in the core of the flow (Figure 14) compared to the experimental data, but remains in a reasonable agreement, and seems to be over-predicted on the heated tube. Near the inner tube, the bubble diameter is underestimated, therefore the interfacial area is overestimated, and then the condensation and the liquid heating are overestimated.

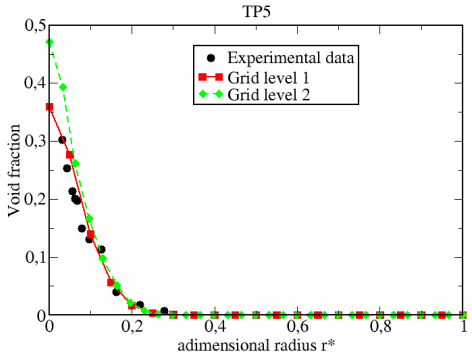

Figure 12: Radial profile of the void fraction.

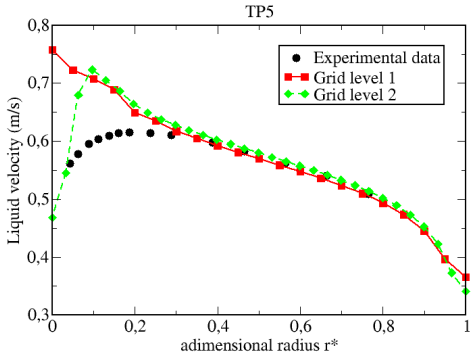

Figure 13: Radial profile of the liquid velocity.

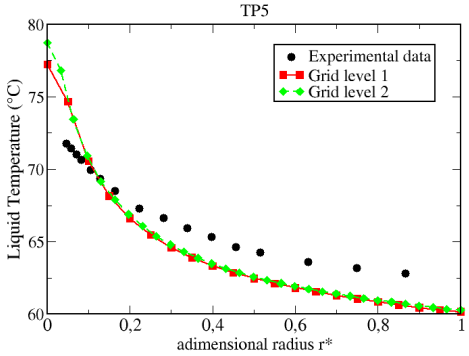

Figure 14: Radial profile of the liquid temperature.

7 Conclusion

The four experiments were computed with NEPTUNE_CFD 1.0.8 with the same set of models. The main objective of this approach is to propose a consistent combination of models, and to evaluate its capabilities to simulate various experimental configurations. The available measurement uncertainties have generally the same order than typical calculation versus measurement discrepancies. The main limitations of the present two-phase CFD can be drawn.

For the adiabatic bubbly flows in a vertical pipe and in a sudden pipe expansion, although the results have acceptable trends, it appears that a polydisperse model for the bubble field does not lead to improvement compared to the monodisperse approach for void fraction prediction. The DEBORA heated tube boiling flow test and ASU boiling flow test in an annulus were simulated. The computed results are quite satisfactory, even if there are not as acceptable as those computed with an imposed diameter for bubbles, given by an experimental observation. It appears that coalescence and break up phenomena play a major role but still remain a challenging task to simulate. However, the

polydisperse approach should be preferred in general since it does not require the knowledge of the experimental mean diameter.

In future validations of NEPTUNE_CFD we intend to add new test cases, which will be based on measurements from new facilities, namely CHAPTAL and TESS. The CHAPTAL experiment provides data on an adiabatic bubbly flow in a vertical pipe. The two-phase mixture is made of water and R116, giving a density ratio comparable to water-steam one in PWR conditions. The TESS installation is designed to provide information on the bulk condensation in a subcooled boiling flow.

ACKNOWLEDGMENTS

This work has been achieved in the framework of the NEPTUNE project, financially supported by CEA (Commissariat à l'Énergie Atomique), EDF, IRSN (Institut de Radioprotection et de Sûreté Nucléaire) and AREVA-NP.

REFERENCES

R. Bel Fdhila, *Analyse expérimentale et modélisation d'un écoulement vertical à bulles dans un élargissement brusque*. PhD Thesis. Institut National Polytechnique de Toulouse. In French (1991)

R. Bel F'Dhila, O. Simonin, "Eulerian prediction of a turburlent bubbly flow downstream of a sudden pipe expansion", *Proc. 6th Workshop on Two-Phase Flow Predictions*, 30 mars-2 avril, Erlangen (1992)

D. Bestion, H. Anglart, B.L. Smith, M. Andreani, J. Mahaffy, D. Lucas, F. Kasahara, E. Komen, P. Mühlbauer, T. Morii, M. Heitsch, F. Moretti, J Ghani Zigh, M. Scheuerer "Extension of CFD Codes to Two-Phase Flow Safety Problems", NEA/CSNI Writing Group, draft6c, (2009)

C.P. Cheung, G.H. Sherman, G.H. Yeoh, J.Y. Tu, "On the numerical study of isothermal vertical bubbly flow using two population balance approaches", *Chemical Engineering Science* 62 4659 – 4674 (2007)

D. Cokljat, M. Slack, S.A. Vasquez, A. Bakker, G. Montante, "Reynolds-Stress Model for eulerian multiphase", *Progress in Computational Fluid Dynamics*, Vol. 6, Nos. 1/2/3 (2006)

J-M. Delhaye, M. Giot, M.L. Riethmuller, *Thermal-hydraulics of two-phase systems for industrial design and nuclear engineering*. Hemisphere and McGraw Hill, 1981

A. Guelfi, D. Bestion, M. Boucker, P. Boudier, P. Fillion, M. Grandotto, J-M. Hérard, E. Hervieu, P. Péturaud, "NEPTUNE - A new software platform for advanced nuclear thermal hydraulics", *Nuclear Science and Engineering*, Vol. 156, pp. 281-324 (2007)

A.Hasan, R.P. Roy, S.P. Kalra, "Experiments on subcooled flow boiling heat transfer in a vertical annular channel", *Int. J. Heat Mass Transfer*, Vol 33, Issue 10, Pages 2285-2293 (1990)

M. Ishii , *Thermo-fluid dynamic, theory of two phase*, Eyrolles, collection de la direction des Etudes et recherches d'Electricité de France, 1975

M. Ishii; "Two-fluid model for two-phase flow", *Multiphase Science and Technology*, Hewitt G.F., Delhaye J.M., Zuber N. Eds., Vol. 5, pp. 1-58 (1990)

B. Končar, E. Krepper, "CFD simulation of convective flow boiling of refrigerant in a vertical annulus", *Nuclear Engineering and Design*, Vol 238, Issue 3, Pages 693-706 (2008)

N; Kurul M.Z. Podowski, "Multidimensional effects in forced convection subcooled boiling", *Proceedings of the Ninth International Heat Transfer Conference Jerusalem*, Israel, pp. 21–26 (1990)

M. Lance, M. Lopez de Bertodano, "Phase distribution phenomena and wall effects in bubbly two-phase flows", *Multiphase Science and Technology*, Vol. 8, Hewitt G.F., Kim J.H., Lahey R.T. Jr., Delhaye J.M. & Zuber N., Eds, Begell House, pp. 69-123 (1994)

T.J. Liu, G. Bankoff, "Structure of air-water bubbly flow in a vertical pipe: II – void fraction, bubble velocity and bubble size distribution", *Int. J. Heat Mass Transfer* Vol 36, Issue 4, pp1061-1072 (1993)

E. Manon, *Contribution à l'analyse et à la modélisation locale des écoulements bouillants sous-saturés dans les conditions des Réacteurs à Eau sous Pression*, PhD thesis, Ecole Centrale Paris, (2000)

N. Méchitoua *et al*., "An unstructured finite volume solver for two-phase water/vapor flows modelling based on an elliptic-oriented fractional step method", *Proc. NURETH-10*, Seoul, Korea, 5-9 October (2003)

S. Mimouni, F. Archambeau, M. Boucker, J. Lavieville, C. Morel, "A second order turbulence model based on a Reynolds stress approach for two-phase boiling flow. Part 1: Application to the ASU-annular channel case", *Nucl. Eng. Des* (2009)

S. Mimouni, F. Archambeau, M. Boucker, J. Lavieville, C. Morel, "A second order turbulence model based on a Reynolds stress approach for two-phase boiling flow and application to fuel assembly analysis", *Nucl. Eng. Des* (2009)

S. Mimouni, F. Archambeau, M. Boucker, J. Laviéville, and C. Morel, "A Second-Order Turbulence Model Based on a Reynolds Stress Approach for Two-Phase Flow. Part I: Adiabatic Cases", *Science and Technology of Nuclear Installations*, Vol 2009, Article ID (2008)

C Morel, J. Pouvreau, J. Laviéville, M. Boucker, "In a sudden expansion with the NEPTUNE code", *3rd International Symposium on two-phase flow modelling and experimentation*, Pisa, September 22-25 (2004)

C. Morel, P. Ruyer, N. Seiler, J. M. Laviéville, "Comparison of several models for multi-size bubbly flows on an adiabatic experiment", *Int. J. Multiphase Flow*, 36, 25-39 (2010)

R.P. Roy, V. Velidandla, S.P. Kalra, P. Péturaud, "Local measurements in the two-phase boiling region of turbulent subcooled boiling flow", *ASME Journal of Heat Transfer* (1993)

P. Ruyer, N. Seiler, M. Beyer, F.P. Weiss, "A bubble size distribution model for the numerical simulation of bubbly flows", *Sixth International Conference on Multiphase Flows, ICMF2007*, Leipzig, Germany (2007)

A. Tomiyama, "Struggle with computational bubble dynamics", *3rd Int. Conf. Multiphase Flow ICMF'98*, Lyon, France, June 8-12 (1998)

H.C. Unal, "Void fraction and incipient point of boiling during the subcooled nucleate flow boiling of water", *International Journal of Heat and Mass Transfer* 20 (1977), 409-419

N. Zuber, "On the dispersed two-phase flow in the laminar flow regime", *Chem. Eng. Sc.*, No. 19, p. 897 (1964)